Electronic Supplementary Information

Label-free and ratiometric detection of microRNA based on target-induced catalytic hairpin assembly and two fluorescent dyes

Danyang Ji,[a] Xi Mou[a] and Chun Kit Kwok*[ab]

[a] *Department of Chemistry, City University of Hong Kong, Kowloon Tong, Hong Kong SAR, China*

[b] *Shenzhen Research Institute of City University of Hong Kong, Shenzhen, 518057, PR China*

** Correspondence: Tel: (852) 3442-6858. Email: ckkwok42@cityu.edu.hk*

Table of contents

Table S1 Sequences of the oligonucleotides used in this work.

Name	Sequence
miRNA-21	5’-UAGCUUAUCAGACUGAUGUUGA-3’
H1	5’-GGGTTTTGGGTCAACATCAGTCTGATAAGCTACCATTGTCACATAGCTTATCAGACTCTACTCATGGGTTTTGGG-3’
H2	5’-TAAGCTATGTGACAATGGTAGCTTATCAGACTCCATTGTCACA-3’
miRNA-125b	5’-UCCCUGAGACCCUAACUUGUGA-3’
H1-2	5’-GGGTTTTGGGTCACAAGTTAGGGTCTCAGGGACCATTGTCACATCCCTGAGACCCTACTACTCATGGGTTTTGGG-3’
H2-2	5’-TCAGGGATGTGACAATGGTCCCTGAGACCCTACCATTGTCACA-3’
TM-miRNA-21[1]	5’-UAGCUUAUCAGACAGAUAUUGA-3’
TM-miRNA-126b[2]	5’-UCCCUGAGACCCUTACUUAUGA-3’
miRNA-765	5’-UGGAGGAGAAGGAAGGUGAUG-3’
miRNA-197	5’-CGGGUAGAGAGGGCAGUGGGAGG-3’
miRNA-432	5’-UCUUGGAGUAGGUCAUUGGGUGG-3’
miRNA-149	5’-AGGGAGGGACGGGGGCUGUGC-3’
miRNA-5196	5’-AGGGAAGGGGACGAGGGUUGGG-3’

[1]Two bases-mismatched miRNA-21

[2]Two bases-mismatched miRNA-125b

Table S2 Comparison of recently reported fluorometric methods for miRNA detection.

Methods	Enzyme	Fluorophore	Target	Linear range	LOD	Method applied	Ref.
DSNSA[a]	duplex-specific nuclease	Malachite green	miRNA-141	0-10 μM	1.03 pM	total RNA	1
DSNSA	duplex-specific nuclease	Malachite green	miRNA-141	1 pM-5 nM	1 pM	Not given	2
SDA[b] and RCA[c]	Klenow Fragment polymerase, Nt.BbvCI nicking endonuclease, T4 DNA ligase, Phi29 DNA polymerase	NMM	let-7b	10 pM-10 nM	3.2 pM	Human serum, total RNA	3
PET[d]-based Amplification-free	Enzyme-free	Ag nanoclusters	miRNA-21	0.1 nM-8 μM	0.06 nM	Total miRNA	4
FRET-based Amplification-free	Enzyme-free	Cyanine-labeled DNA probe	miRNA-20	0.05-0.75 nM	0.03 nM	Calf serum	5
CHA	Enzyme-free	2-aminopurine labeled DNA probe and Thioflavin T	miRNA-122	0.5-50 nM	72 pM	Cell lysate	6
CHA	Enzyme-free	Ag nanoclusters	miRNA-141	0-200 nM	0.2971 nM	Human serum	7
CHA	Enzyme-free	2-aminopurine labeled DNA probe	miRNA-21	4 pM-40 nM	4 pM	Cell lysate	8
CHA	Enzyme-free	NMM and DAPI	miRNA-21	10 pM-45 nM	3.1 pM	Cell lysate	This work

[a] Duplex-specific nuclease signal amplification; [b] Strand-displacement amplification; [c] Rolling circle amplification; [d] Photoinduced electron transfer

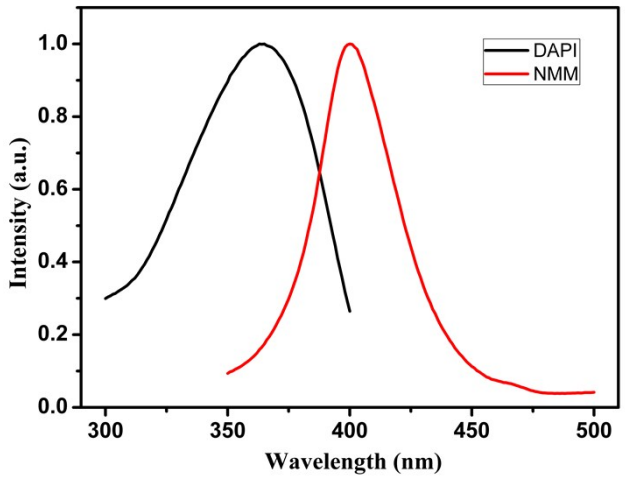

Fig. S1 Excitation spectra of DAPI (500 nM) and NMM (500 nM) in the presence of H1 (150 nM) and H2 (200 nM). The excitation intensity was normalized to 1.

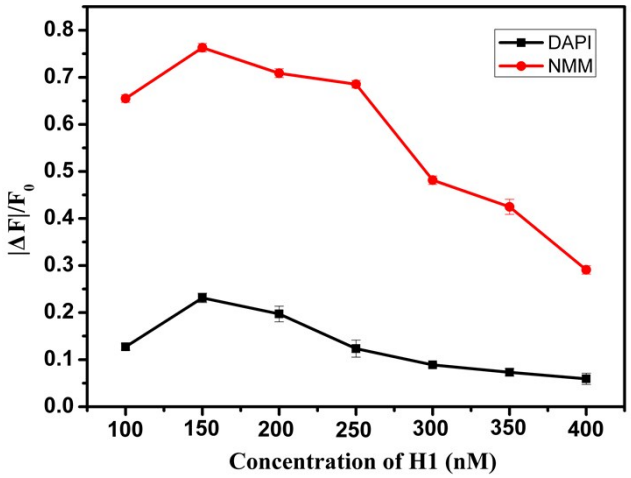

Fig. S2 Optimization of the concentration of H1. The concentration of miRNA-21 is 45 nM, H2 is 200 nM, DAPI is 100 nM, NMM is 1 μM. $\Delta F=F-F_0$, F and F_0 are the fluorescence intensity in the presence and absence of miRNA-21, respectively. The error bar represents the standard deviation of three independent replicates. According to the figure, 150 nM H1 was chosen for further investigation to ensure the highest signal-to-background ratio.

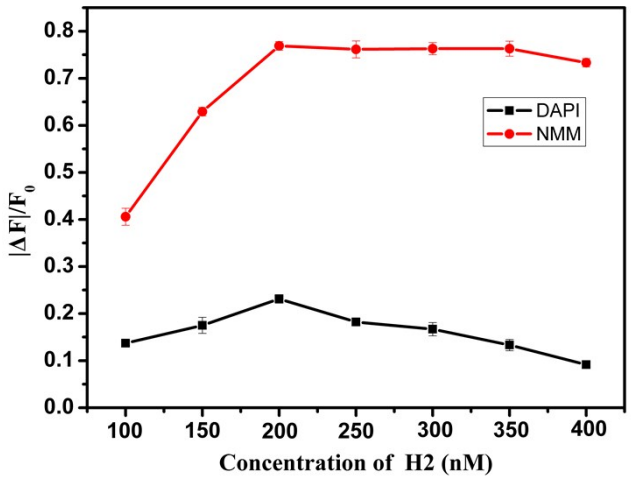

Fig. S3 Optimization of the concentration of H2. The concentration of miRNA-21 is 45 nM, H1 is 150 nM, DAPI is 100 nM, NMM is 1 μM. $\Delta F=F-F_0$, F and F_0 are the fluorescence intensity in the presence and absence of miRNA-21, respectively. The error bar represents the standard deviation of three independent replicates. According to the figure, 200 nM H2 was chosen for further investigation to ensure the highest signal-to-background ratio.

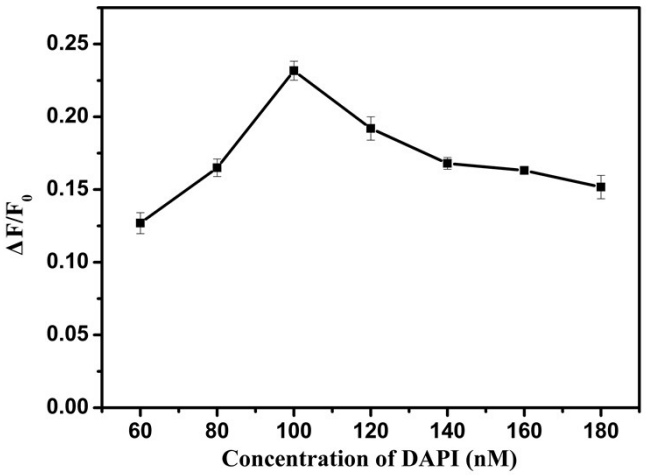

Fig. S4 Optimization of the concentration of DAPI. The concentration of miRNA-21 is 45 nM, H1 is 150 nM, H2 is 200 nM. $\Delta F=F-F_0$, F and F_0 are the fluorescence intensity in the presence and absence of miRNA-21, respectively. The error bar represents the standard deviation of three independent replicates. According to the figure, 100 nM DAPI was chosen for further investigation to ensure the highest signal-to-background ratio.

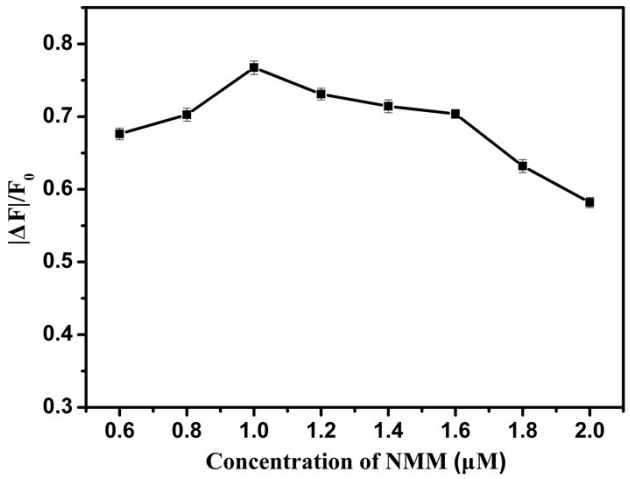

Fig. S5 Optimization of the concentration of NMM. The concentration of miRNA-21 is 45 nM, H1 is 150 nM, H2 is 200 nM. $\Delta F=F-F_0$, F and F_0 are the fluorescence intensity in the presence and absence of miRNA-21, respectively. The error bar represents the standard deviation of three independent replicates. According to the figure, 1 μM NMM was chosen for further investigation to ensure the highest signal-to-background ratio.

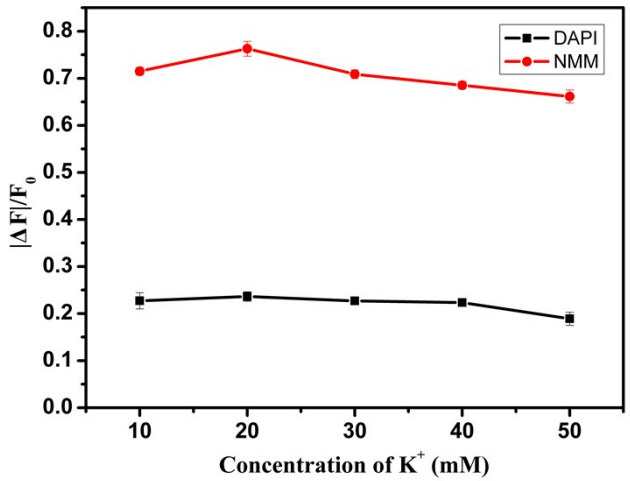

Fig. S6 Optimization of the concentration of K^+. The concentration of miRNA-21 is 45 nM, H1 is 150 nM, H2 is 200 nM, DAPI is 100 nM, NMM is 1 μM. $\Delta F=F-F_0$, F and F_0 are the fluorescence intensity in the presence and absence of miRNA-21, respectively. The error bar represents the standard deviation of three independent replicates. According to the figure, 20 mM K^+ was chosen for further investigation to ensure the highest signal-to-background ratio.

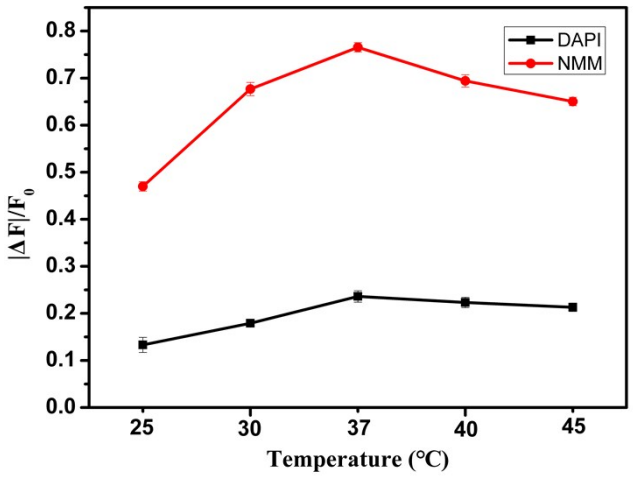

Fig. S7 Optimization of the incubation temperature. The concentration of miRNA-21 is 45 nM, H1 is 150 nM, H2 is 200 nM, DAPI is 100 nM, NMM is 1 μM. $\Delta F=F-F_0$, F and F_0 are the fluorescence intensity in the presence and absence of miRNA-21, respectively. The error bar represents the standard deviation of three independent replicates. According to the figure, 37°C was chosen for further investigation to ensure the highest signal-to-background ratio.

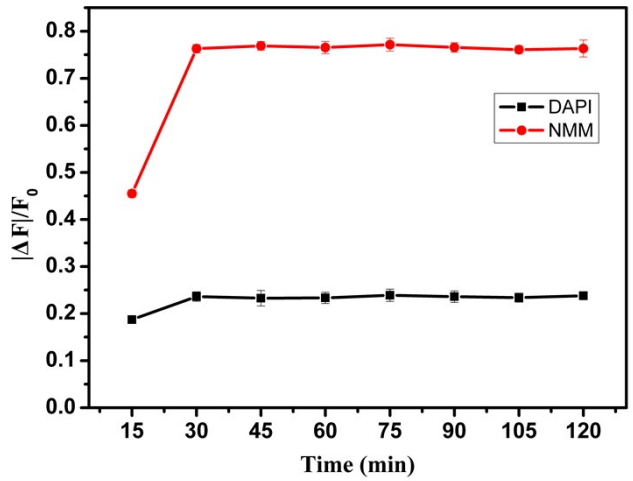

Fig. S8 Optimization of the incubation time of the catalytic hairpin assembly (CHA) process. The concentration of miRNA-21 is 45 nM, H1 is 150 nM, H2 is 200 nM, DAPI is 100 nM, NMM is 1 μM. $\Delta F=F-F_0$, F and F_0 are the fluorescence intensity in the presence and absence of miRNA-21, respectively. The error bar represents the standard deviation of three independent replicates. According to the figure, an incubation time of 30 min was chosen for CHA reaction to ensure the highest signal-to-background ratio.

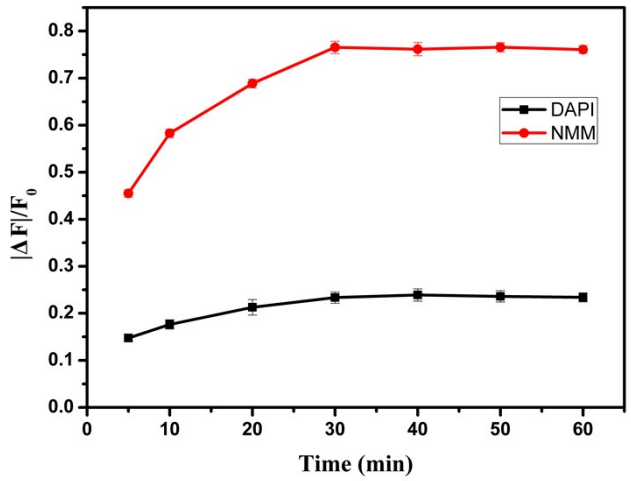

Fig. S9 Optimization of the incubation time of DAPI and NMM. The concentration of miRNA-21 is 45 nM, H1 is 150 nM, H2 is 200 nM, DAPI is 100 nM, NMM is 1 μM. $\Delta F=F-F_0$, F and F_0 are the fluorescence intensity in the presence and absence of miRNA-21, respectively. The error bar represents the standard deviation of three independent replicates. According to the figure, an incubation time of 30 min was chosen for DAPI and NMM to ensure the highest signal-to-background ratio.

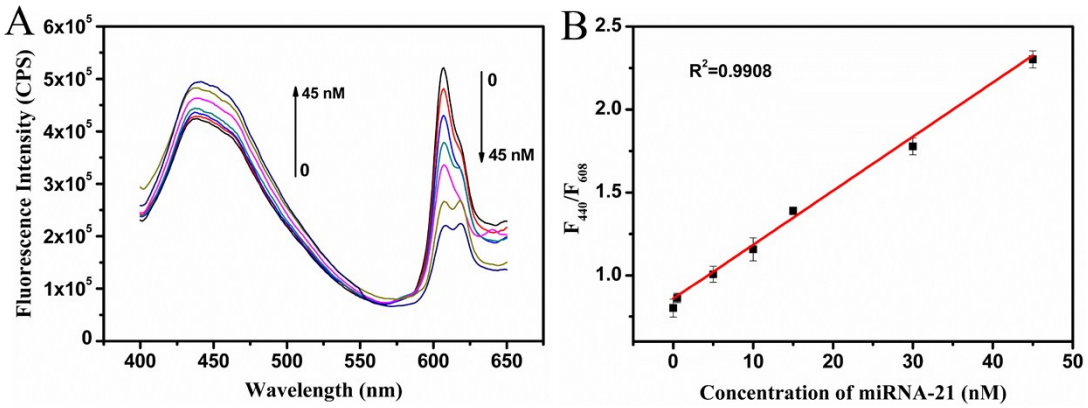

Fig. S10 MicroRNA-21 detection in HeLa cell lysate. (A) Fluorescence emission spectra of the system with different concentrations of miRNA-21 (0-45 nM). (B) Scatter plot of F_{440}/F_{608} as a function of the concentrations of miRNA-21 (0-45 nM). F_{440} and F_{608} are the fluorescence signals of DAPI and NMM, respectively. The error bar represents the standard deviation of three independent replicates. The new shoulder that appeared at NMM fluorescence peak was likely owing to the influence from autofluorescence of cell components and the binding of cell components to NMM.

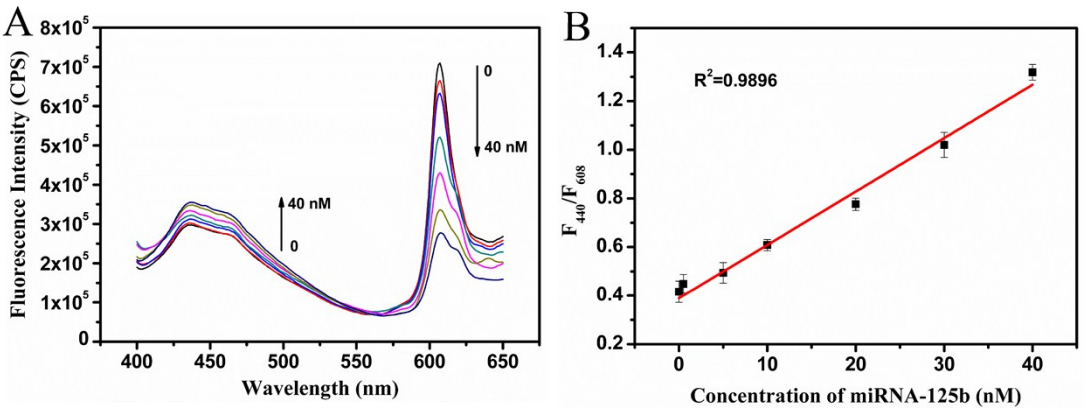

Fig. S11 MicroRNA-125b detection in HeLa cell lysate. (A) Fluorescence emission spectra of the system with different concentrations of miRNA-21 (0-40 nM). (B) Scatter plot of F_{440}/F_{608} as a function of the concentrations of miRNA-125b (0-40 nM). F_{440} and F_{608} are the fluorescence signals of DAPI and NMM, respectively. The error bar represents the standard deviation of three independent replicates. The new shoulder that appeared at NMM fluorescence peak was likely owing to the influence from autofluorescence of cell components and the binding of cell components to NMM.

References

1. K. Zhang, K. Wang, X. Zhu, F. Xu and M. Xie, *Biosens. Bioelectron.*, 2017, **87**, 358-364.
2. H. Zhou, C. Yang, H. Chen, X. Li, Y. Li and X. Fan, *Biosens. Bioelectron.,* 2017, **87**, 552-557.
3. R. Wang, L. Wang, H. Zhao and W. Jiang, *Biosens. Bioelectron.,* 2016, **86**, 834-839.
4. S. Lu, S. Wang, J. Zhao, J. Sun and X. Yang, *Anal. Chem.*, 2017, **89**, 8429-8436.
5. Z. Jin, D. Geissler, X. Qiu, K. D. Wegner and N. Hildebrandt, *Angew. Chem. Int. Ed*., 2015, **54**, 10024-10029.
6. Y. Liu, T. Shen, J. Li, H. Gong, C. Chen, X. Chen and C. Cai, *ACS Sens.*, 2017, **2**, 1430-1434.
7. H. Kim, S. Kang, K. S. Park and H. G. Park, *Sens. Actuators, B*, 2018, **260**, 140-145.
8. S. Li, C. Liu, H. Gong, C. Chen, X. Chen and C. Cai, *Talanta*, 2018, **178**, 974-979.